Femtosecond laser writing of waveguide retarders in fused silica for polarization control in optical circuits

Luís A. Fernandes[1,2], Jason R. Grenier[1], Peter R. Herman[1], J. Stewart Aitchison[1] and Paulo V. S. Marques[2]

[1]*Institute for Optical Sciences, and the Department of Electrical and Computer Engineering University of Toronto, 10 Kings College Rd., Toronto, Ontario, M5S 3G4, Canada*

[2]*INESC-Porto, Departamento de Física e Astronomia da Universidade do Porto, Rua do Campo Alegre 687, 4169-007 Porto, Portugal*

lfernandes@fc.up.pt

Abstract: Femtosecond laser (300 fs, 500 kHz, 522 nm) fabrication of optical waveguides in bulk silica glass is extended to waveguide retarders. We study the merits of nanograting orientation (perpendicular or parallel to the waveguide) for generating high and low birefringence waveguides. This is used together with other exposure condition to control the waveguide birefringence between 10^{-5} and 10^{-4} permitting for the simultaneous fabrication of the waveguides and the tuning of the retardance demonstrating quarter and half-wave retarders in the 1200 nm to 1700 nm spectrum. The wavelength dependence of the birefringence is also characterized over a range of exposure conditions.

OCIS codes: (130.3120) Integrated optics devices; (130.5440) Polarization-selective devices; (140.3390) Laser materials processing.

References and links

1. S. Nolte, M. Will, J. Burghoff, and A. Tuennermann, "Femtosecond waveguide writing: a new avenue to three-dimensional integrated optics," Appl. Phys. A-Mater. **77,** 109–111 (2003).
2. A. M. Kowalevicz, V. Sharma, E. P. Ippen, J. G. Fujimoto, and K. Minoshima, "Three-dimensional photonic devices fabricated in glass by use of a femtosecond laser oscillator," Opt. Lett. **30,** 1060–1062 (2005).
3. S. Eaton, W. Chen, H. Zhang, R. Iyer, J. Li, M. Ng, S. Ho, J. S. Aitchison, and P. R. Herman, "Spectral Loss Characterization of Femtosecond Laser Written Waveguides in Glass With Application to Demultiplexing of 1300 and 1550 nm Wavelengths," J. Lightwave Technol. **27,** 1079–1085 (2009).
4. Y. Bellouard, T. Colomb, C. Depeursinge, M. Dugan, A. Said, and P. Bado, "Nanoindentation and birefringence measurements on fused silica specimen exposed to low-energy femtosecond pulses," Opt. Express **14,** 8360–8366 (2006).
5. V. R. Bhardwaj, P. B. Corkum, D. M. Rayner, C. Hnatovsky, E. Simova, and R. S. Taylor, "Stress in femtosecond-laser-written waveguides in fused silica," Opt. Lett. **29,** 1312–1314 (2004).
6. M. Ams, G. Marshall, and M. Withford, "Study of the influence of femtosecond laser polarisation on direct writing of waveguides," Opt. Express **14,**, 13158–13163 (2006).
7. S. Eaton, H. Zhang, M. Ng, J. Li, W. Chen, S. Ho, and P. R. Herman, "Transition from thermal diffusion to heat accumulation in high repetition rate femtosecond laser writing of buried optical waveguides," Opt. Express **16,** 9443–9458 (2008).
8. P. Yang, G. R. Burns, J. Guo, T. S. Luk, and G. A. Vawter, "Femtosecond laser-pulse-induced birefringence in optically isotropic glass", J. Appl. Phys. **95,** 5280 (2004).
9. E. Bricchi, B. Klappauf, and P. Kazansky, "Form birefringence and negative index change created by femtosecond direct writing in transparent materials," Opt. Lett. **29,** 119–121 (2004).

10. R. Taylor, C. Hnatovsky, E. Simova, P. Rajeev, D. Rayner and P. Corkum, "Femtosecond laser erasing and rewriting of self-organized planar nanocracks in fused silica glass," Opt. Lett. **32,** 2888–2890 (2007).
11. Y. Shimotsuma, M. Sakakura, P. Kazansky, M. Beresna, J Qiu, K. Miura and K. Hirao, "Ultrafast Manipulation of Self-Assembled Form Birefringence in Glass," Advanced Materials **22,** 4039–4043 (2010).
12. G. Cheng, K. Mishchik, C. Mauclair, E. Audouard, and R. Stoian, "Ultrafast laser photoinscription of polarization sensitive devices in bulk silica glass," Opt. Express **17,** 9515–9525 (2009).
13. W. Cai, A. R. Libertun, and R. Piestun, "Polarization selective computer-generated holograms realized in glass by femtosecond laser induced nanogratings," Opt. Express **14,** 3785–3791 (2006).
14. D. Papazoglou and M. Loulakis, "Embedded birefringent computer-generated holograms fabricated by femtosecond laser pulses," Opt. Lett. **31,** 1441–1443 (2006).
15. M. Beresna and P. G. Kazansky, "Polarization diffraction grating produced by femtosecond laser nanostructuring in glass," Opt. Lett. **35,** 1662–1664 (2010).
16. L. Ramirez, M. Heinrich, S. Richter, F. Dreisow, R. Keil, A. Korovin, U. Peschel, S. Nolte, and A. Tunnermann, "Tuning the structural properties of femtosecond-laser-induced nanogratings," Appl. Phys. A-Mater. **100,** 1–6 (2010).
17. M. Lobino and J. L. O'Brien, "Entangled photons on a chip," Nature **469,** 43–44 (2011).
18. G. Marshall, A. Politi, J. Matthews, P. Dekker, M. Ams, M. Withford, and J. O'Brien, "Laser written waveguide photonic quantum circuits," Opt. Express **17,** 12546–12554 (2009).
19. L. Sansoni, F. Sciarrino, G. Vallone, P. Mataloni, A. Crespi, R. Ramponi, and R. Osellame, "Polarization Entangled State Measurement on a Chip," Phys. Rev. Lett. **105,** 200503 (2010).
20. A. Politi, M.J. Cryan, J.G. Rarity, S. Yu, J.L. O'Brien, "Silica-on-silicon waveguide quantum circuits," Science **320,** 5876, 646–649 (2008).
21. L. A. Fernandes, J. R. Grenier, P. R. Herman, J. S. Aitchison and P. V. S. Marques, "Femtosecond laser fabrication of birefringent directional couplers as polarization beam splitters in fused silica," Opt. Express **19,** 11992–11999 (2011).
22. S. Betti, G. De Marchis, and E. Iannone, "Polarization modulated direct detection optical transmission systems," J. Lightwave Technol. **10,** 1985–1997 (1992).
23. C. H. Bennett and G. Brassard, "Quantum Cryptography: Public Key Distribution and Coin Tossing," in Proceedings of the IEEE International Conference on Computers, Systems and Signal Processing, Bangalore, India, 1984 (IEEE, New York,1984), 175–179;IBM Tech. Discl. Bull. 28, 31533163 (1985).
24. J. L. O'Brien, A. Furusawa and J. Vuckovic, "Photonic quantum technologies," Nature Photonics **3,** 687, 687–695 (2009).
25. J. L. O'Brien, "Optical quantum computing," Science **318,** 1567–1570 (2007).
26. L. Shah, A. Arai, S. Eaton, and P. R. Herman, "Waveguide writing in fused silica with a femtosecond fiber laser at 522 nm and 1 MHz repetition rate," Opt. Express **13,** 1999–2006 (2005).
27. H. Zhang, S. Eaton, and P. R. Herman, "Single-step writing of Bragg grating waveguides in fused silica with an externally modulated femtosecond fiber laser," Opt. Lett. **32,** 2559–2561 (2007).

1. Introduction

Femtosecond laser technologies have enabled prospects of producing three-dimensional integrated optical circuits in a single writing step [1-3]. Fused silica is a widely favored material in femtosecond laser processing due to formation of low loss and stable optical devices. Waveguides fabricated with femtosecond laser exposure have shown asymmetric geometries where stresses have been associated with birefringence and propagation losses [4-6]. Unlike the more symmetric waveguides generated in borosilicate glass [7], it has been shown that the birefringence formed in fused silica waveguides under certain femtosecond fabrication conditions [8] depends strongly on both the polarization of the writing laser and the intensity of the writing beam that contributes to strong birefringence according to the orientation of laser-induced nanogratings [9-12]. These nanograting effects have been studied and used for the formation of computer generated holograms [13, 14], polarization diffraction gratings [15], and birefringent elements [16], and the use of this technology for 5D optical storage has been suggested [11].

By carefully controlling the laser exposure parameters, such as pulse energy, scanning speed and polarization, the waveguide birefringence can be controlled and applied to fabricate polarization dependent devices. Such devices have recently been proposed [17] for application in integrated quantum entanglement experiments [18, 19] where beam splitters have been formed in bulk fused silica or borosilicate as an alternative to lithographic processing of silica-on-silicon

optical circuits [20].

An integrated polarization beam splitting waveguide has been recently demonstrated [21] using this approach. In this paper, we further extend the laser fabrication of polarization dependent waveguide devices by demonstrating controlled polarization retardance in the 1200 nm to 1700 nm wavelength region. Such devices open the possibility to integrate, using a single fabrication step, polarization splitters and waveguide wave plates in bulk glass, such that more complex and highly stable polarization devices can be integrated into three-dimensional optical circuits. Such polarization control is further required for differential polarization phase-shift keying in optical communication [22], quantum key distribution [23, 24] for cryptography applications and quantum computing [25].

2. Fabrication

The waveguides were fabricated using a Yb-doped fiber, chirped pulse amplified system (IMRA America µJewel D-400-VR), frequency doubled to 522 nm center wavelength, as described in [26]. Exposure conditions tested were with a 300 fs pulse width, 500 kHz repetition rate and pulse energy varied between 80 nJ and 200 nJ. The beam was focused 75 µm below the surface of the fused silica substrates (Corning 7980, 50.8 mm $\times$ 25.4 mm $\times$ 1 mm with all faces optically polished) with a 0.55 NA aspheric lens which produced a spot with a diameter of 1.6 µm ($1/e^2$ intensity). The sample was scanned at a constant speed of 0.27 mm/s using an air-bearing motion stage (Aerotech ABL1000) with a resolution of 2.5 nm, to produce a 24.5 mm long waveguide parallel with the short edge of the sample.

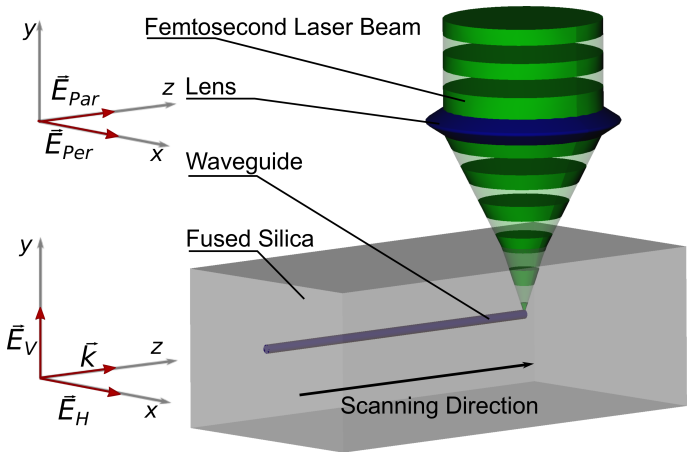

Fig. 1. Schematic diagram of the waveguide fabrication where E_{Par} and E_{Per} represent the parallel and perpendicular polarizations of the writing laser respectively. E_V and E_H indicate the electric field orientation of Vertical, V, and Horizontal, H, waveguide polarization modes, respectively.

The polarization state at the focus was oriented with a half-wave plate in the laser path to be either parallel (along the z-axis) or perpendicular (along the x-axis) with respect to the scanning direction as shown in Fig. 1, manipulating the form birefringence induced by the laser generated nanogratings.

Bragg grating waveguides (BGW) were fabricated with the same exposure setup with the addition of an acousto-optic modulator (AOM) in the laser path as described in [27]. Controlling the AOM frequency from 595 Hz to 470 Hz provided tuning of the Bragg reflection peak from 1300 nm to 1650 nm.

3. Characterization methods

The birefringence of the waveguides was determined by two complementary techniques that both use free space, end-fire, coupling of broadband light into the end facet of the waveguide with an aspheric objective lens (New Focus, 30X, 0.4 NA).

In the first approach, the spectral splitting of the Bragg resonance in the BGWs was measured between the two perpendicular polarization modes as designated by, vertical, V (along the y-axis, slow axis, corresponding to the TM mode) and, horizontal, H (along the x-axis, fast axes, corresponding to the TE mode), as defined in Fig. 1 yielding the result in Fig. 2. This spectral splitting was measured with an Optical Spectrum Analyzer (OSA, Ando 6317B) set at 0.01 nm resolution for a broadband light source (Agilent 83437A, 1300 nm to 1600 nm). The polarization was controlled by rotating a broadband polarizer (Thorlabs LPNIR). Following the Bragg relation $\lambda_B = 2n\Lambda$, where λ_B is the reflected Bragg wavelength, n is the effective index of the mode and Λ is the period of the grating, one can obtain the waveguide birefringence, $\Delta n = n_v - n_h$, according to Equation (1).

$$\Delta n = \frac{\Delta\lambda_B}{2\Lambda} \tag{1}$$

Here, $\Delta\lambda_B$ is the difference between the Bragg resonance of the vertically and horizontally polarized modes which are the proper axes of the waveguide.

A second, more accurate, measurement of the waveguide birefringence was made by using the crossed polarizers method. A broadband unpolarized light source was launched into a waveguide after passing a linear polarizer oriented at 45° with respect to the x-axis (Fig. 1) while an OSA set to a resolution of 2 nm measured the waveguide output after passing a second broadband linear polarizer in two orientations of 45° and 135°.

The total waveguide output power, $P_o = P_{pm} + P_{cm}$, is split into parallel power P_{pm} and crossed power P_{cm} components measured at the respective 45° and 135° analyzer positions that depend on the waveguide retardance, $\delta = 2\pi\Delta nL/\lambda$, according to Equations (2) and (3) where the normalized powers P_p and P_c are defined.

$$P_p = \frac{P_{pm}}{P_o} = \frac{1}{2}(1+\cos\delta) \tag{2}$$

$$P_c = \frac{P_{cm}}{P_o} = \frac{1}{2}(1-\cos\delta) \tag{3}$$

A similar birefringence analysis was presented in [8]. The retardance introduced by the waveguide can then be determined from Equation (4) within an ambiguous phase order of $m = 0,1,2,3,...$ to yield a birefringence, Δn, as calculated by Equation (5), where, λ is the wavelength and L is the waveguide length.

$$\delta = \pm\arccos(P_p - P_c) + m2\pi \tag{4}$$

$$\Delta n = \frac{\delta\lambda}{2\pi L} \tag{5}$$

The $m2\pi$ phase ambiguity and the $\pm$ sign in the arccosine function of the crossed polarizers method (Equations (4)) can be solved by the less precise method of Bragg grating resonance splitting (Equation (1)) which scales linearly with the waveguide birefringence.

To account for the mode mismatch when assessing the propagation losses of the waveguides the intensity profile of the modes propagating in the waveguides was recorded by coupling the

light from a tunable laser (Photonetics Tunics-BT) with a single mode fiber (SMF) to the waveguides and imaging the output onto a CCD camera (Spiricon SP-1550M) by a 60X magnification lens.

4. Results

Laser exposure conditions in a range of 90 nJ to 160 nJ pulse energy for parallel writing polarization yielded waveguides having moderately low propagation losses, α, (0.3 dB/cm to 1.4 dB/cm) with a mode field diameter (MFD) matched to the 10.4 µm MFD in SMF-28 fiber as indicated in Table 1, as a function of the pulse energy for 1550 nm wavelength probing. In Table 2, waveguide data for writing with a perpendicular laser polarization produces similar values of MFD but with 6-fold higher propagation loss for the best waveguides. The propagation losses were adjusted for the small mode mismatch loss shown in Table 1 and Table 2. The difference between the MFD for vertical and horizontal polarized modes is less than the 0.5 µm uncertainty in the measurements.

Table 1. Waveguide properties for various pulse energy exposure for parallel polarization of the writing laser

Pulse Energy (nJ)	MFD (x, y) (µm)	Mismatch loss (dB)	Prop. loss, α (dB $\cdot$ cm^{-1})
90	11.2, 11.7	0.04	1.4
130	9.0, 10.2	0.05	0.3
160	8.5, 10.2	0.09	0.6

Table 2. Waveguide properties for various pulse energy exposure for perpendicular polarization of the writing laser

Pulse Energy (nJ)	MFD (x, y) (µm)	Mismatch loss (dB)	Prop. loss, α (dB $\cdot$ cm^{-1})
90	Poor guiding	Poor guiding	Poor guiding
130	11.1, 11.8	0.04	2.4
160	12.1, 12.7	0.14	1.9

Figure 2 shows the transmission spectra of two BGWs written with parallel (along z-axis) and perpendicular (along x-axis) polarization of the writing laser and spectrally probed with vertical (along y-axis) and horizontal (along x-axis) input polarized light. The birefringence present in the waveguides, Δn, can be calculated directly form the spectral splitting, $\Delta\lambda$ from Equation (1). Birefringence values of $(4.7 \pm 0.5) \times 10^{-5}$ and $(1.7 \pm 0.1) \times 10^{-4}$ were found for the examples in Fig. 2 for parallel and perpendicular writing laser polarizations, respectively. Here the BGWs spectral response was relatively strong, introducing up to a 30% discrepancy between the birefringence values calculated with the BGW splitting method on segmented waveguides and the values determined with the crossed polarizers technique on continuous waveguides.

For the 1550 nm BGWs, the perpendicular polarization of the writing laser shows a greater birefringence due to the strong form birefringence associated with this nanograting orientation but with a higher propagation loss as seen by comparing Table 1 with Table 2.

Figure 3 shows the experimentally measured values of the normalized transmission for the parallel (P_p) and crossed (P_c) powers using a 45° linear polarized input. The values for the transmitted waveguide power, P_p and P_c, measured with the crossed polarizer technique and calculated based on Equations (2) and (3), respectively, are shown in Fig. 3 as a function of the

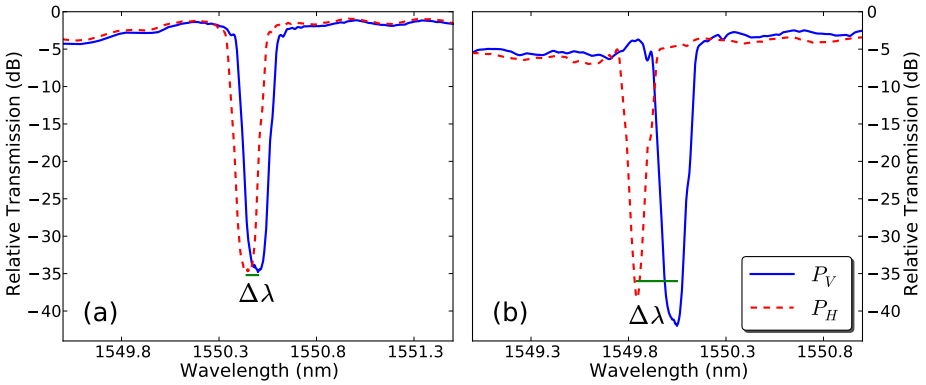

Fig. 2. Transmission spectra of two BGWs written with parallel (a) and perpendicular (b) polarizations of the writing laser with 160 nJ pulse energy and probed with vertical polarized modes (– blue solid line) and horizontal polarized modes (- - red dashed line).

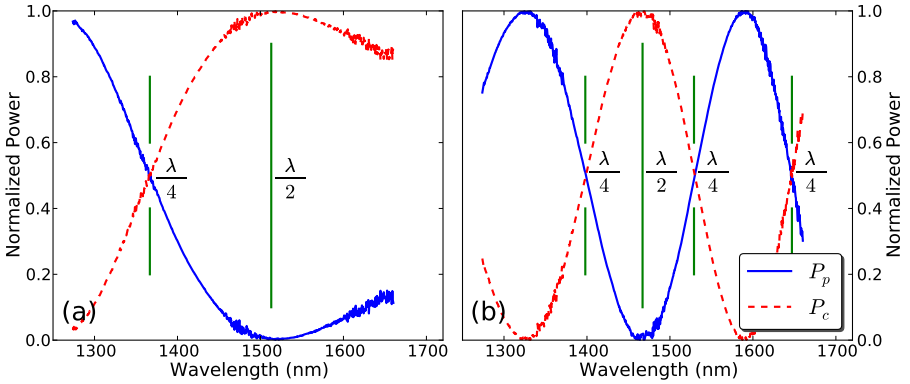

Fig. 3. Normalized spectrum for P_p (– blue solid line) and P_c (- - red dashed line) for (a) parallel and (b) perpendicular polarizations of the writing laser with 160 nJ pulse energy and for 45° linearly polarized input light. The $\lambda/4$ and $\lambda/2$ markers indicate wavelengths where the waveguide operates as a quarter-wave and half-wave retarder.

wavelength. The waveguides operate as a half-wave plate as indicated in the figure when the value of P_c is 1 and the value for P_p is 0 for linearly polarized input light along 45° in respect to the proper axes. The quarter-wave plate conditions are also identified for the case when both P_p and P_c are equal (0.5 in Fig. 3). For parallel polarization writing (Fig. 3a) a half-wave plate is noted at 1513 nm and a quarter-wave plate is noted at 1365 nm. Strong form birefringence in the perpendicular polarization case (Fig. 3b) yields a half-wave plate at 1467 nm and three quarter-wave plates at 1400 nm, 1530 nm, and 1646 nm.

Birefringence values assessed from the Bragg grating polarization splitting are plotted across the 1300 nm to 1650 nm spectrum in Fig. 4a together with the birefringence values calculated from Equations (4) and (5) from the data of the crossed polarizers technique in Fig. 3.

The phase ambiguity of Equations (4) was resolved definitively by adjusting the sign and order, m, for all wavelengths to match the calculated data with the Bragg grating data. The 1×10^{-5} discrepancy between data from the two methods, which is attributed to the physical difference of continuous versus segmented waveguides, is smaller than the phase adjustment (sign and order m) discrepancy of up to 5×10^{-5} in birefringence, thus providing non-

ambiguous phase determination for the crossed polarizers data.

There is a significant difference in the birefringence values ranging from 1×10^{-5} to 5×10^{-5} for parallel writing in contrast with values of 1.6×10^{-4} to 2.2×10^{-4} for perpendicular writing laser polarizations, where exposure conditions of 160 nJ pulse energy and 0.27 mm/s constant scanning speed were used in both cases.

Figure 4b demonstrates the strong dependence of waveguide birefringence on the laser pulse energy for the parallel polarization exposure. The birefringence appears strongest (7×10^{-5}) at lower exposures (90 nJ and 110 nJ), however, the trends over a larger spectrum suggest that the waveguide birefringence reaches a maximum at a specific wavelength that shifts to lower values for decreasing laser pulse energy.

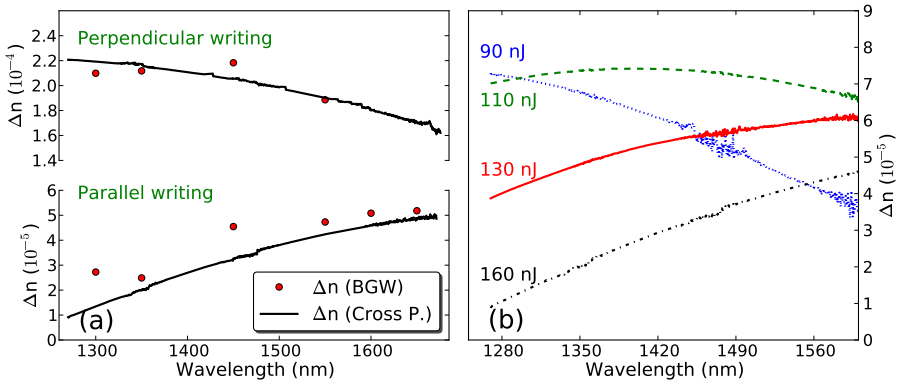

Fig. 4. Birefringence as a function of the wavelength for (a) perpendicular and parallel polarizations of the writing laser with 160 nJ pulse energy and 0.27 mm/s scanning speed (averaged over 5 samples) and (b) various laser pulse energies for parallel polarized writing at 0.27 mm/s scanning speed.

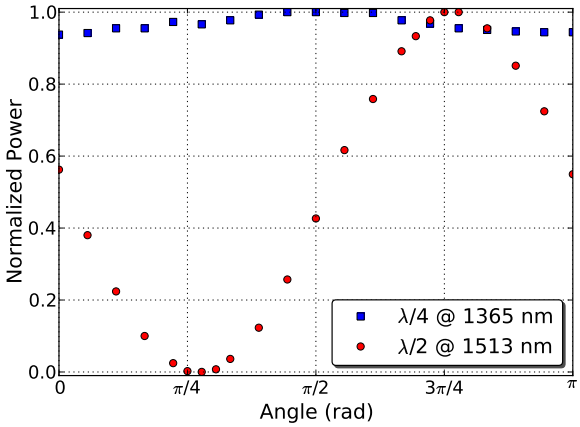

Fig. 5. Polarization analyzer response of a quarter-wave (■ blue square) and a half-wave plate (● red circle) response of a 25.4 cm long waveguide fabricated with parallel polarization writing at 160 nJ pulse energy.

Using linear polarized input at 45°, with approximately 5 mW power from the broadband source, the waveguide characterized in Fig. 3a was analyzed with a linear polarizer as a function

of output angle yielding the quarter-wave and the half-wave plots at 1365 nm and 1513 nm, respectively, as shown in Fig. 5.

The 95% to 100% power variation at 1365 nm is very close to the ideal quarter-wave plate operation, while the output at 1513 nm shows the expected sinusoidal power variation with linear polarized light output at $3\pi/4$ angle having 35 dB contrast to the power measured with orthogonal polarization at $\pi/4$ angle.

5. Discussion

As shown in Fig. 4, the waveguide birefringence varies strongly with wavelength and can favor the fabrication of a broadband wave retarder. Such a device requires a linear increase in the birefringence (Δn) with respect to the wavelength such that the retardance (δ) remains constant over a given band. This condition is available for the case of 110 nJ pulse energy in Fig. 4b, where a half-wave plate with 9.06 mm waveguide length and a quarter-wave plate with 4.53 mm length are expected with a 65 nm band centered at 1283 nm and within a phase variation of $\pm$ 0.005 rad. Further tuning of the exposure condition may allow us to broaden and extend such wave plates to other spectral windows. The wave plates were heated from 20 °C to 70 °C with no measurable change in birefringence. Therefore, the wave plates are stable for probe intensities low enough not to produce significant changes in temperature.

For the present 25.4 mm long waveguides, the wave retarders formed with parallel polarization of the writing laser were zero-order ($m = 0$) wave plates (Fig. 5), while the wave plates fabricated with perpendicular polarization of the writing laser were third-order and fourth-order wave plates. In the former case, the total insertion loss of the device was 1.5 dB while in the latter case, a zero-order half-wave plate would only require approximately a 4 mm long waveguide at 1550 nm wavelength that has much more favorable 0.8 dB insertion loss. Therefore, perpendicular polarization of the writing laser is preferred for making more compact and lower loss wave plates, but this advantage may be less favorable depending on the laser pulse energy (Fig. 4b) and required MFD of the waveguide that is also dependent on the laser pulse energy.

More generally, the data presented here demonstrated that quarter-wave and half-wave plate waveguides can be optimized for a given wavelength to offer low loss, mode matching, and short insertion length. With this femtosecond fabrication technique, it is possible to insert specific retardance on-the-fly at key positions in optical circuits or produce low and high birefringence waveguides for arbitrary tuning of its polarization dependence characteristics.

6. Conclusion

We successfully demonstrated the first laser formed buried optical waveguides behaving as discrete quarter-wave and half-wave plates. A 35 dB polarization contrast was found for a half-wave plate while there was only a 5% power variation for a quarter-wave plate. In this paper, we further demonstrated two complementary techniques to accurately measure the birefringence in femtosecond laser formed waveguides and used these techniques to study the birefringence dependence on wavelength and exposure conditions. These wave plate devices may prove to be important for future integration into optical circuits required in quantum entanglement experiments and on-a-chip quantum optics applications.

7. Acknowledgments

The authors would like to acknowledge the Natural Sciences and Engineering Research Council of Canada and Canadian Institute for Photonic Innovations for the financial support of this project. Luís Fernandes would also like to acknowledge the Portuguese Fundação para a Ciência e Tecnologia for his Ph.D Fellowship.